Cell Metabolism
Resource

A ^{13}C Isotope Labeling Strategy Reveals the Influence of Insulin Signaling on Lipogenesis in *C. elegans*

Carissa L. Perez[1,2] and Marc R. Van Gilst[1,*]
[1]Division of Basic Sciences, Fred Hutchinson Cancer Research Center, Seattle, WA 98109, USA
[2]Molecular and Cellular Biology Program, University of Washington, Seattle, WA 98195, USA
*Correspondence: vangilst@fhcrc.org
DOI 10.1016/j.cmet.2008.08.007

SUMMARY

Although studies in *C. elegans* have identified numerous genes involved in fat storage, the next step is to determine how these factors actually affect in vivo lipid metabolism. We have developed a ^{13}C isotope assay to quantify the contribution of dietary fat absorption and de novo synthesis to fat storage and membrane lipid production in *C. elegans*, establishing the means by which worms obtain and process fatty acids. We applied this method to characterize how insulin signaling affects lipid physiology. Several long-lived mutations in the insulin receptor gene *daf-2* resulted in significantly higher levels of synthesized fats in triglycerides and phospholipids. This elevation of fat synthesis was completely dependent upon *daf-16*/FoxO. Other long-lived alleles of *daf-2* did not increase fat synthesis, however, suggesting that site-specific mutations in the insulin receptor can differentially influence longevity and metabolism, and that elevated lipid synthesis is not required for the longevity of *daf-2* mutants.

INTRODUCTION

In addition to behavioral and environmental factors, it is clear that genetic background plays a substantial role in determining the propensity for obesity and related complications. Consequently, there is considerable interest in defining genes that affect the partitioning of dietary nutrients for fat storage. Studies in *C. elegans* have characterized numerous pathways that modulate lipid accumulation, including insulin/IGF, serotonin, tubby, and nuclear receptor signaling (Mukhopadhyay et al., 2005; Ogg et al., 1997; Sze et al., 2000; Van Gilst et al., 2005). Furthermore, a genome-wide RNAi screen isolated over 300 genes that influence total fat accumulation (Ashrafi et al., 2003).

In principle, genes could alter fat storage by modulating three factors: (1) how much fatty acid is ingested and absorbed from the diet, (2) how much dietary nutrient is converted to fat via de novo lipogenesis, and (3) how much fat is expended through β-oxidation. Because little is known about these processes in nematodes, the ability to elucidate the mechanisms of fat regulatory genes in *C. elegans* has been limited. For example, mutation of the insulin receptor gene, *daf-2*, can increase life span and fat storage through inappropriate activation of the FoxO transcription factor DAF-16. Microarray studies have shown that the DAF-2 receptor, through regulation of DAF-16, controls the expression of numerous genes predicted to participate in fatty acid metabolism, but it is still not clear how DAF-2 and its regulatory targets actually modulate fat synthesis, absorption, and/or expenditure (Halaschek-Wiener et al., 2005; McElwee et al., 2003; Murphy et al., 2003).

The question of how *C. elegans daf-2* regulates lipid metabolism is of particular interest given its potential to inform us about how insulin signaling controls longevity. Like *C. elegans*, knockout of the insulin receptor increases longevity in mice (Holzenberger et al., 2003; Katic et al., 2007; Kenyon et al., 1993). The conservation of metabolic regulation, however, is less clear, as the effect of insulin signaling on fat storage in mammals appears to vary based on tissue and context (Bluher et al., 2002; Bruning et al., 1998, 2000); consequently, defining the relationship between insulin receptor control of lipid metabolism and longevity, in both *C. elegans* and mammals, requires further study.

In order to better understand the mechanisms by which the insulin receptor and related genes regulate lipid physiology in *C. elegans*, it is essential to develop methods for characterizing and quantifying fatty acid metabolism. Stable isotope-based experiments have been employed to monitor fatty acid flux in numerous biological systems (Brunengraber et al., 1997; Kelleher, 2004; McCabe and Previs, 2004; Murphy, 2006; Strawford et al., 2004). Furthermore, isotope labeling of food has been applied to globally monitor macronutrient partitioning in an invertebrate model organism, *Drosophila* (Min et al., 2006; O'Brien et al., 2008). Here, we present a ^{13}C isotope-labeling approach to characterize dietary fat absorption and fatty acid synthesis in *C. elegans* and to determine how insulin signaling influences these central aspects of lipid metabolism.

RESULTS

A ^{13}C Enrichment Strategy to Identify and Quantify Dietary and Synthesized Fatty Acids

We designed a "mixed isotope" assay to quantify the relative contributions of de novo synthesis and dietary fat absorption to total lipid composition in *C. elegans* (Figure 1A). In principle, animals that are fed a mixture (~1:1) of ^{13}C-enriched *E. coli* (OP50) and unlabeled bacteria should obtain approximately half of their nutrients from ^{13}C-labeled bacteria and half of their nutrients from unlabeled ^{12}C bacteria. Therefore, using this strategy, fats absorbed from the diet and directly incorporated into

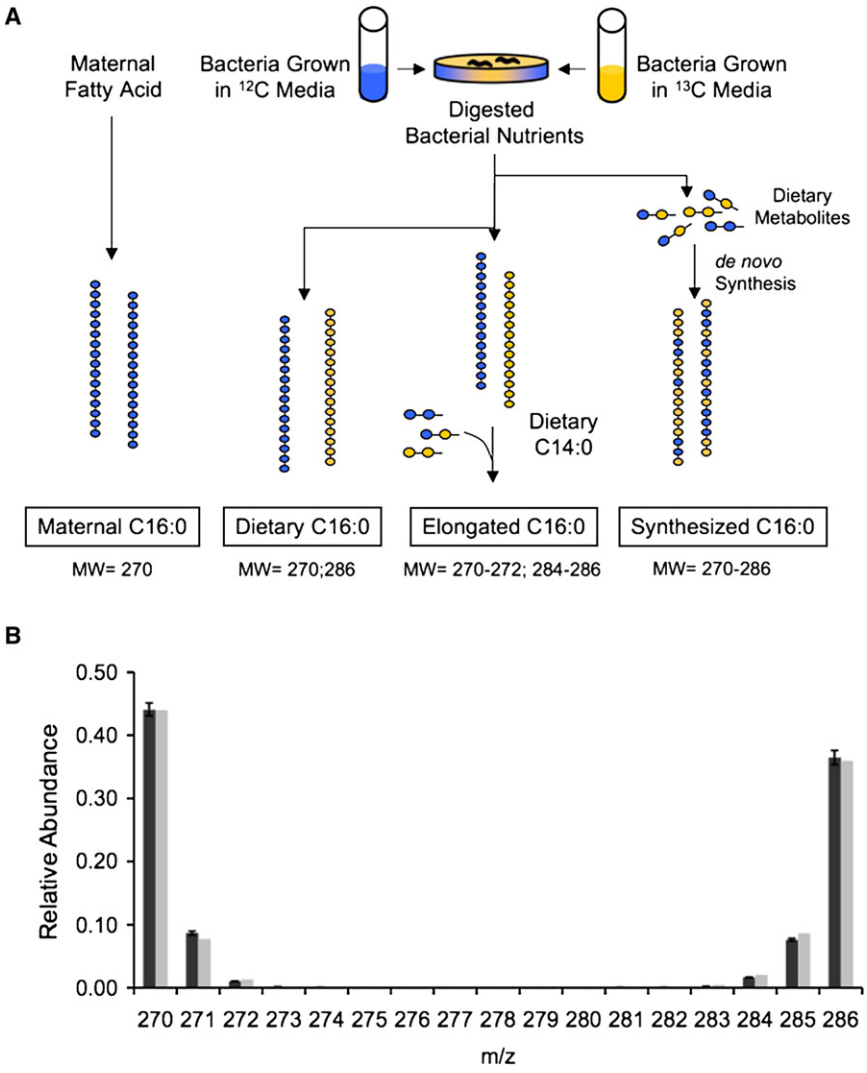

Figure 1. "Mixed Isotope" Labeling Strategy

(A) *C. elegans* palmitate (C16:0) can be obtained from four distinct sources, and by feeding worms a 1:1 mixture of ^{12}C- and ^{13}C-enriched bacteria each of these sources will produce fatty acids with a specific MW signature. Because we subsequently analyze fatty acid methyl esters, the MW for each C16:0 isotopomer reflects that of the corresponding methyl ester. Directly absorbed C16:0 will either be fully unlabeled (MW = 270) or fully labeled (MW = 286). C16:0 produced in *C. elegans* from elongation of dietary C14:0 will involve fusion of a fully unlabeled or fully labeled 14-carbon backbone with labeled, partially labeled, or unlabeled acetyl-CoA; consequently, C16:0 created by elongation of C14:0 will generate isotopomers ranging from MW = 270–272 and MW = 284–286. Third, fatty acids synthesized de novo from dietary metabolites will have a statistical distribution of C16:0 isotopomers ranging from MW = 270–286 that depends on the isotope composition of the acetyl-CoA pool. Fourth, maternally inherited palmitate will be fully unlabeled (MW = 270).

(B) Mass spectra of C16:0 obtained from bacteria on control feeding plates were averaged (n = 11) and are displayed here as mean fraction of total abundance (± standard deviation [SD]). The peak at 270 Daltons represents C16:0 from bacteria grown in fully unlabeled media, and the peak at 286 Daltons represents C16:0 from bacteria grown in ^{13}C-labeled media. The gray bars represent calculation of isotopomer peaks resulting from natural ^{13}C isotope in unlabeled media (1.11%) and ^{12}C isotope impurity in the ^{13}C media (284 and 285). Importantly, the absence of detectable peaks between 272 and 284 Daltons shows that no mixing of isotope label occurred on the feeding plates.

worm lipids will either be fully composed of ^{13}C (if directly obtained from labeled bacteria) or fully composed of ^{12}C (if absorbed from unlabeled bacteria). In contrast, fats synthesized de novo in *C. elegans* will contain a mixture of ^{12}C and ^{13}C since synthesis substrates will be derived from the breakdown of labeled and unlabeled bacterial nutrients. The relative contributions of dietary fatty acid absorption and de novo synthesis can therefore be quantified by analyzing the molecular weight (MW) distribution of purified fatty acids.

We prepared mixed isotope "feeding plates" by plating a 1:1 mixture of bacteria grown in standard unlabeled media and bacteria grown in ^{13}C-enriched media (Isogro). To confirm the isotope composition of the fatty acids in our feeding plates, and to ensure that there was no crosscontamination during the labeling assay, we independently analyzed bacterial fatty acids from the feeding plates for each experiment. Figure 1B shows an averaged mass spectrum of palmitate (C16:0) obtained from bacteria washed off of mixed label feeding plates. It is clear from these data that there are no quantifiable peaks in the "synthesized region" of the mass spectrum. The shoulder peaks present at 271–272 and 284–285 are a consequence of natural ^{13}C abundance or ^{12}C contamination in our ^{13}C bacterial growth media. In nature, ^{12}C is 98.9% abundant, and the probability of incorporating ^{13}C into a palmitate methyl ester was determined using a binomial distribution (Kelleher, 2001). Similarly, we calculated the isotope purity of our ^{13}C bacteria enrichment by comparing the fractional abundance of the isotopic peaks at 284 and 285 Daltons (Figure 1B). On average, we found that the ^{13}C enrichment of our Isogro media was 98.5%. These data confirmed that for the period in which the bacteria reside on the feeding plates, there was no detectable incorporation of contaminating carbon sources, other than natural isotope variation. Thus, dietary fatty acids available to worms grown on mixed isotope feeding plates were either 98.5% composed of ^{13}C or 98.9% composed of ^{12}C.

We first applied our technique to characterize C16:0 synthesis and absorption. The mass spectrum of C16:0, obtained from worms grown on a mixed isotope feeding plate, revealed C16:0 species with a range of MWs (isotopomers), from 270 Daltons (for a palmitate methyl ester fully composed of ^{12}C) to 286 Daltons (for a palmitate methyl ester fully composed of ^{13}C) (Figure 2A). To derive a quantitative model to fit these data, we considered that C16:0 was obtained from four sources (Figure 1A). First, dietary

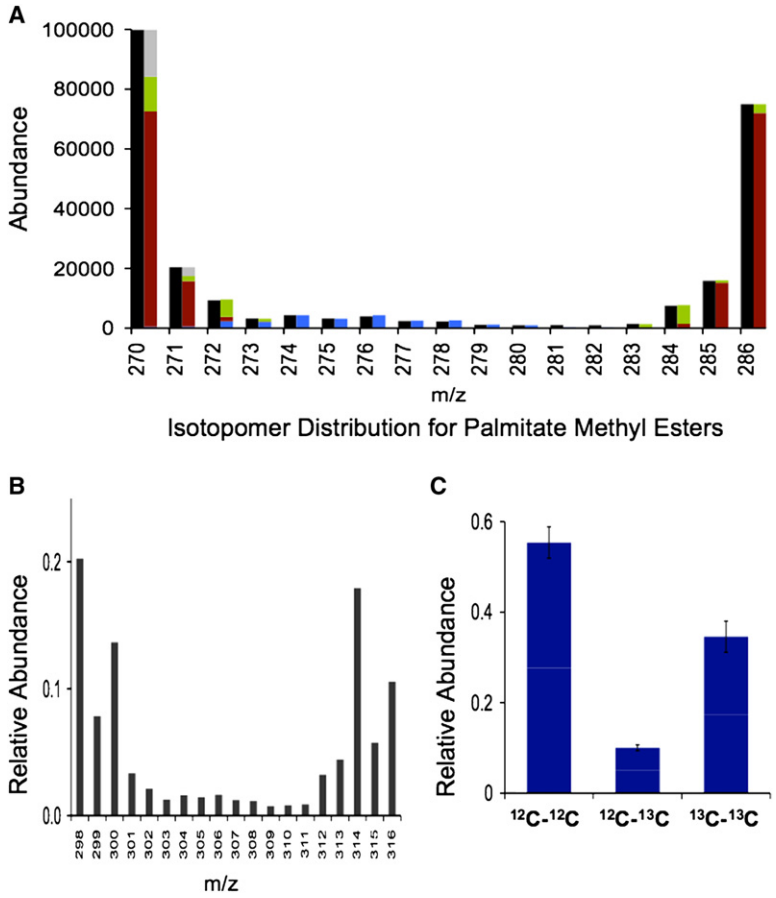

Figure 2. Characterization of Palmitate Absorption and Synthesis

(A) A mass spectrum of C16:0 methyl ester obtained from the total lipid of worms grown on a mixed isotope diet from the L1 to the L4 stage of larval development (black). In order to model these data, we accounted for (1) dietary fat absorption (red), (2) de novo synthesis (blue), (3) elongation of dietary fat (green), and (4) maternal contribution (gray). Our analysis also accounted for shoulder peaks due to natural ^{13}C abundance in the unlabeled media and ^{12}C isotope impurity in the ^{13}C media.

(B) A mass spectrum of stearate (C18:0) obtained from L4 larvae that had been grown on mixed label feeding plates from the L1 stage of development.

(C) By examining the relative abundance of isotopomer peaks at 314, 315, and 316 Daltons, we calculated the probability of incorporating unlabeled (^{12}C-^{12}C), partially labeled (^{12}C-^{13}C), and fully labeled (^{13}C-^{13}C) acetyl-CoA isotopomers. Data are the compilation of three experiments and are presented as the mean ± SD.

absorption: intact C16:0 taken up from unlabeled bacteria and incorporated into worm lipids displayed a MW of 270 Daltons, whereas C16:0 directly absorbed from ^{13}C-enriched bacteria contributed to the isotopomer peak at 286 Daltons (shoulder peaks due to isotope impurities were accounted for in our analysis) (Figure 2A). Second, C16:0 could be formed in *C. elegans* by elongation of dietary C14:0; molecules generated in this fashion would fall between 270–272 Daltons and 284–286 Daltons. Third, C16:0 could be derived from de novo synthesis; fatty acids produced by synthesis will display an isotope-labeling pattern that falls into a trinomial distribution, which will depend on the probability of incorporating acetyl-CoA units that are ^{12}C-^{12}C, ^{12}C-^{13}C, or ^{13}C-^{13}C (See Experimental Procedures). Although these probabilities could be determined by fitting the isotopomer data, we were able to independently determine the acetyl-CoA isotopomer distribution by measuring the elongation of C16:0 to C18:0 (Figure 2C). Finally, since our assays were carried out by placing unlabeled larvae (L1 stage) on mixed isotope bacteria, maternally derived C16:0 that remains in harvested L4 stage animals also contributed to the isotopomer peak at 270 Daltons.

Taking into account these four possible sources of palmitate, we derived a mathematical model to fit the mass distribution (Figure 2A, see Experimental Procedures for a description of the data analysis). Our model revealed that the majority of *C. elegans* C16:0 was derived from direct absorption of bacterial fatty acid. However, de novo synthesis did account for ~7% of total palmitate.

Origin of Other *C. elegans* Fatty Acid Species

Our findings revealed that dietary fat absorption is the primary source of worm palmitate; however, *C. elegans* contains numerous other fatty acids, some of which are not found in its bacterial diet (Table S1 available online). Stearate (C18:0), oleate (C18:1n9), linoleate (C18:2n6), and several 20 carbon polyunsaturated fats are not available in the common laboratory diet (*E. coli* [OP50]) and must be obtained by elongation and desaturation of C16:0 (Figure 3) (Watts and Browse, 2002). Although synthesis accounted for only ~7% of the steady-state levels of C16:0, we found a more predominant role for de novo synthesis in the production of MUFAs and PUFAs (up to ~19% of total fatty acid) (Figure 3). Twenty carbon fatty acids could not be assessed by our method due to extensive fragmentation of these molecules in the mass spectrometer.

We also found that *C. elegans* monomethyl branched-chain fatty acids (mmBCFAs), C15ISO and C17ISO, were >99% derived from de novo synthesis. mmBCFAs are not present in the OP50 diet and cannot be produced from modification of bacterial fatty acids. For these reasons, it has been proposed that mmBCFAs must be derived from de novo synthesis (Kniazeva et al., 2004); our results provide direct biochemical confirmation of this hypothesis. In contrast, four *C. elegans* fatty acid species, vaccenate (C18:1n7), palmitoleate (C16:1n7), and two cyclopropane fatty acids (C17Δ and C19Δ), are prevalent dietary fats. We found that ~95% of C18:1n7 and C16:1n7 and >99% of the cyclopropyl fatty acids originate from direct absorption of the bacterial fatty acid (Figure 3).

Disruption of Insulin Signaling Leads to Increased De Novo Fatty Acid Synthesis

We next defined the impact of insulin signaling on fatty acid synthesis. Worms harboring the commonly studied *e1370* allele of *daf-2* contained a >2-fold higher proportion of synthesized fatty acids (Figure 4A). Because *daf-2(e1370)* animals have elevated fat storage, we considered the possibility that synthesis was

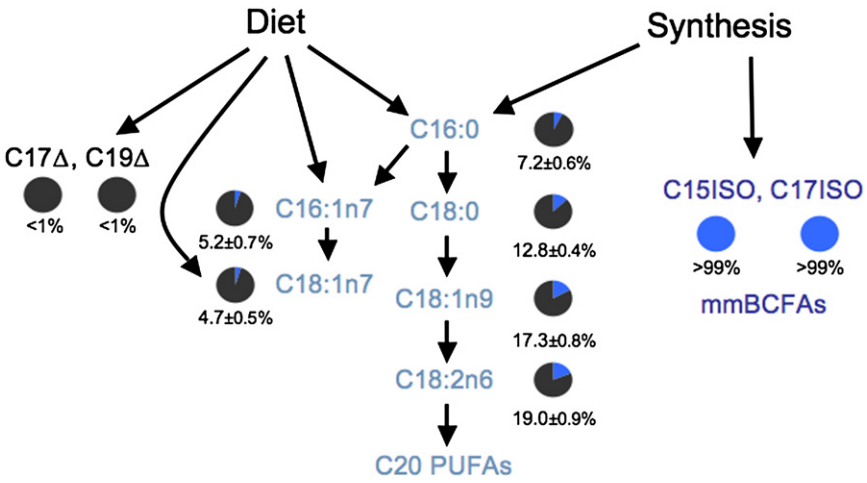

Figure 3. Biosynthetic Origin of *C. elegans* Lipids

The most abundant *C. elegans* fatty acids are shown here along with their biosynthetic origins. The proportion of fatty acid derived from synthesis is represented in blue in the pie graphs and numerically indicated below. Fatty acid obtained from absorption and/or modification of dietary fatty acid is displayed in gray. Data represent the compilation of five experiments and are displayed as the mean ± standard error of the mean (SEM).

specifically increased in these animals and directly allocated to TAG production. To address this question, we analyzed the relative abundance of synthesized and dietary fatty acids in triglycerides (TAGs) and phospholipids (PLs). We found that wild-type (WT) animals displayed a similar fraction of synthesized and dietary fatty acids in both lipid types; furthermore the *daf-2(e1370)* mutation resulted in a higher proportion of synthesized fatty acids in both TAGs and PLs (Figure 4B). This result implies that synthesized and absorbed fatty acids contribute to a common pool that feeds both membrane synthesis and fat storage. Thus, in *daf-2(e1370)* mutants, more synthesized fatty acid is available for PL production and for TAG storage.

A higher fraction of synthesized fatty acid might not necessarily reflect an absolute increase in de novo synthesis but rather a reduced contribution of dietary fat to the total lipid pool. This scenario, however, would result in less total fat storage. Under our conditions, we found approximately 80% higher levels of TAGs in *daf-2(e1370)* animals (Figure 4C). These data are consistent with previous reports, which implemented different strategies to show a similar impact of *daf-2(e1370)* mutation on fat storage (Ashrafi et al., 2003; Hellerer et al., 2007; Ogg et al., 1997). We next determined how much of the elevated fat storage observed in *daf-2(e1370)* animals originated from de novo synthesis. When broken down into synthesized and absorbed components, it is clear that there are ~3-fold higher levels of synthesized fatty acids in *daf-2(e1370)* TAGs than in WT TAGs (Figure 4C). This increased supply of synthesized fatty acids is sufficient to account for a significant proportion (>60%) of the elevated fat storage in *daf-2(e1370)* mutants. *daf-2(e1370)* mutants also contain higher levels of dietary fatty acids in their TAGs. Much of this increase is likely due to the fact that more dietary fatty acid is free for TAG storage because of the larger contribution of synthesized fat to PL production. However, because increased fatty acid synthesis often inhibits fatty acid β-oxidation via malonyl-CoA, it is probable that reduced β-oxidation is also a factor in *daf-2(e1370)* worms.

Alternative *daf-2* Alleles Have Distinct Impacts on Fatty Acid Synthesis

In addition to the *daf-2(e1370)* mutation, other long-lived alleles of *daf-2* have been isolated that result in site-specific amino acid substitutions in different domains of the receptor (Gems et al., 1998; Patel et al., 2008). Although these alleles all cause life-span extension, they have variable impacts on other aspects of worm physiology, including reproduction, pharyngeal pumping, and motility. We found that several of these alleles displayed dramatically different effects on lipogenesis. Specifically, we found two *daf-2* alleles that did not affect fatty acid synthesis, two alleles that caused a moderate increase in synthesis, and one allele that stimulated fatty acid synthesis as strongly as *daf-2(e1370)* (Figure 4D). We confirmed that all of these *daf-2* alleles led to increased life span under our experimental conditions (see Figure S3). The level of fatty acid synthesis observed in the different *daf-2* mutants also correlated with TAG storage, further supporting the conclusion that the elevated fat storage caused by *daf-2* mutation is primarily due to changes in de novo synthesis (Figure 4E).

Insulin Regulation of Fatty Acid Synthesis Depends on DAF-16/FoxO

The impact of insulin signaling on longevity is dependent upon downstream activation of the DAF-16/FoxO transcription factor (Kenyon et al., 1993). In WT animals, the insulin receptor activates a signaling cascade that phosphorylates DAF-16/FoxO and prevents its localization to the nucleus (Lee et al., 2001). Deletion of *daf-16* is sufficient to suppress the longevity of *daf-2* mutants. We found that the effect of the *daf-2(e1370)* mutation on fatty acid synthesis was also completely dependent upon *daf-16*, as a *daf-2(e1370);daf-16(m26)* double mutant displayed levels of fatty acid synthesis that were slightly lower than that of WT animals. Furthermore, mutation of *daf-16(m26)* alone resulted in a slight reduction in de novo synthesis (Figure 4D). Taken together, these results imply that *daf-16* stimulates de novo synthesis, and that activation of the insulin signaling pathway represses de novo synthesis, at least in part, by inhibition of *daf-16*.

DISCUSSION

Using a ^{13}C isotope-labeling strategy, we provided a thorough description of how *C. elegans* obtains and distributes fatty acids. Elegant stable isotope approaches have been used to measure lipid metabolism in other animal models including humans; what distinguishes this method, however, is that the entire carbon component of a natural food source is labeled, enabling simultaneous monitoring of fatty acid absorption, elongation and

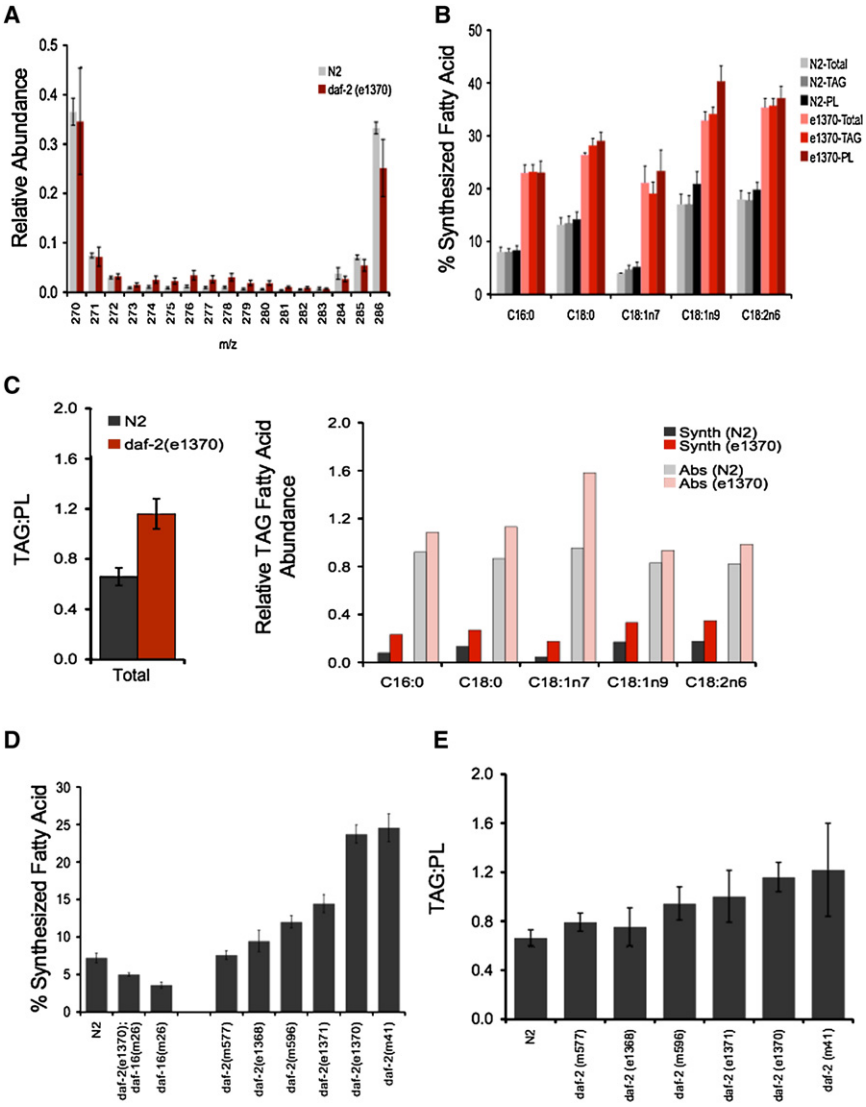

Figure 4. Regulation of Fatty Acid Synthesis and TAG Storage by *daf-2*

(A) Isotopomers exclusively associated with de novo synthesis (MW 274–280) are increased in palmitate isolated from the total lipid of the *daf-2(e1370)* animals (red), as compared to WT animals (gray). Data are the mean of five experiments ± SD.

(B) The percentage of fatty acids derived from de novo synthesis in phospholipid (PL), TAG (triacylglyceride), and total lipid is shown for WT (N2) and *daf-2(e1370)*. Data are presented as the mean of three experiments ± SEM.

(C) The total amount of TAG in N2 and *daf-2(e1370)* mutants. Data are displayed as mean TAG:PL ratio ± SEM. For each fatty acid, we used total TAG measurements along with fatty acid synthesis data to estimate the relative abundance of dietary (Abs) and synthesized fatty acid in the TAG of N2 and *daf-2(e1370)* animals.

(D) The relative amount of de novo synthesis in various *daf-2* and *daf-16* mutants. Data presented here are for palmitate; however a similar pattern was observed for most other fatty acid species (data not shown). Data represent the mean of at least five experiments ± SEM.

(E) TAG measurements in WT and *daf-2* mutants. Numbers shown represent the mean of at least five experiments ± SEM.

desaturation, and de novo synthesis. Thus, multiple aspects of nutrient utilization and lipid metabolism can be examined in a single assay with an exceptional degree of detail and precision. Additionally, this approach can survey metabolism over the entire course of development and adulthood; thus, the long-term impact of genetic mutations and dietary manipulations can be readily assessed in high-throughput fashion. We expect this general strategy to be applicable for investigating many different metabolic pathways in *C. elegans,* as well as other model organisms.

We found that worm fatty acids are derived from four sources: (1) direct absorption and incorporation of dietary fats, (2) absorption and modification of dietary fats by elongation and/or desaturation, (3) de novo synthesis, and (4) maternal inheritance. When grown on the OP50 strain of *E. coli*, a standard laboratory diet, the majority of fatty acids are directly obtained from ingested bacteria. However, de novo synthesis is not a negligible factor, contributing especially to species not available in the diet, such as C18:0 (~13%), C18:1n9 (~17%), C18:2n6 (~19%), and mmBCFAs (>99%). Presumably, worms will modify fatty acid synthesis and absorption patterns to accommodate food sources with different lipid compositions. The fact that the relative contribution of de novo synthesis and dietary fat absorption was similar in PLs and TAGs implies that dietary and synthesized fats freely diffuse through the worm such that a common pool is used for the majority of PL and TAG synthesis.

There has been considerable interest in the *C. elegans* insulin receptor due to its influence on longevity, stress resistance, and lipid storage (Kenyon et al., 1993; McElwee et al., 2006; Wolkow et al., 2000). The commonly studied *daf-2(e1370)* allele blocks insulin signaling, extends life span, and leads to elevated fat accumulation. We found that *daf-2(e1370)* animals have more than double the amount of synthesized fatty acids in TAG and PL, implying that de novo synthesis is the predominant mechanism by which the insulin signaling pathway affects fat storage in *C. elegans*. This conclusion is further supported by a positive correlation between the fatty acid synthesis levels of different *daf-2* mutants and their total fat storage.

Our results with alternative *daf-2* alleles also show that the impacts of the insulin receptor on life span and lipogenesis are genetically separable. Thus, the enhanced longevity of *daf-2* mutants does not require increased lipid synthesis. Furthermore, the fact that *daf-16* is required for both longevity and elevated fat synthesis suggests that *daf-16* might respond differently to distinct *daf-2* mutations, such that some mutations activate its capacity to promote longevity but not de novo lipogenesis (Figure 5A). This could occur because differential modification

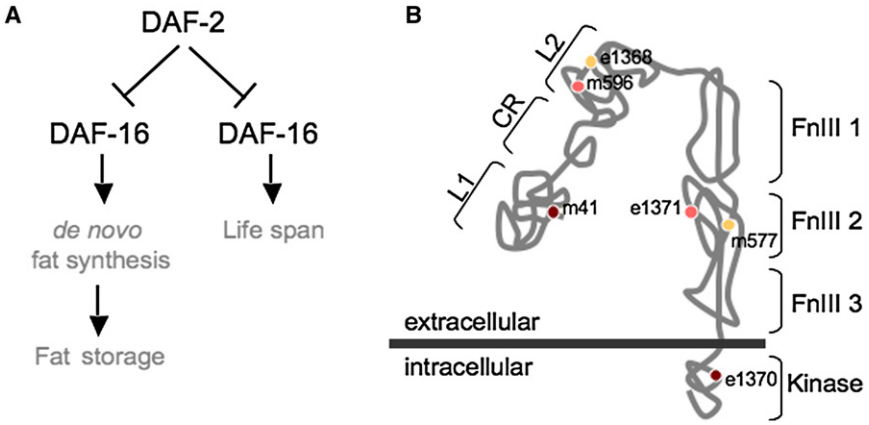

Figure 5. Insulin Signaling Mutants Differentially Impact Lipogenesis

(A) Our findings demonstrate that insulin signaling suppresses de novo synthesis by inhibiting the lipogenic function of DAF-16/FoxO. Some alleles of *daf-2* increase de novo lipogenesis and enhance longevity, whereas other *daf-2* alleles lead to *daf-16*-dependent longevity but do not cause stimulation of de novo synthesis. Thus, site-specific mutations in the insulin receptor gene can differentially affect longevity and lipogenesis, implying that the downstream mechanisms utilized to generate these physiological outcomes are, at least partially, distinct.

(B) The predicted locations of the *daf-2* alleles used in this study are displayed on a structural diagram of the insulin receptor. The cartoon is based on alignment of the DAF-2 protein with the human insulin receptor (Patel et al., 2008).

of *daf-16* is required for its impact on lipogenesis, because of tissue-specific differences in the signaling mechanism, or because *daf-16* control of lipogenesis may be more sensitive to signaling dosage. Alternatively, the effect of the *daf-2(e1370)* mutation on lipogenesis may involve an additional factor that functions together with *daf-16* to stimulate fatty acid synthesis. In this case, some *daf-2* alleles may not influence this additional factor.

The structural position of the *daf-2* alleles studied here does not provide a clear explanation for their distinct effects on longevity and lipid synthesis (Figure 5B). The two alleles with the strongest enhancement of de novo synthesis are *m41* and *e1370*. The *e1370* mutation localizes near the active site of the kinase domain, where it could potentially interfere with downstream signaling. The *m41* allele localizes to the L1 domain, which is responsible for ligand interaction; however *m41* does not alter an amino acid predicted to make direct contact with the insulin ligand. The *m577* and *e1371* mutations both localize to the FnIII2 domain, but only one of these alleles affects de novo synthesis. Furthermore, *m596* and *e1368* localize to the L2 domain but also impact lipid synthesis differently. Both the FnIII2 domain and L2 domain reside in the extracellular portion of the insulin receptor and do not directly participate in ligand binding or kinase interaction. Thus, these *daf-2* mutations may directly disrupt interaction with an undefined factor or may indirectly alter ligand binding or kinase activation by differentially perturbing allosteric changes. Alternatively, *daf-2* alleles may have distinct impacts on protein stability, thus varying the strength of the insulin response. Further genetic and structural investigation will be necessary to establish how these simple site-specific mutations distinctly affect DAF-16/FoxO activity, longevity, and lipogenesis. In any event, the fact that we were able to identify insulin receptor mutants that specifically impacted life span, but not metabolism, suggests that targeted mutations in the insulin receptor may be able to manipulate distinct physiological outcomes; such a finding warrants further investigations in *C. elegans* and mammalian models.

EXPERIMENTAL PROCEDURES

Growth on Mixed Isotope Feeding Plates

To prepare mixed isotope feeding plates, separate ^{12}C- and ^{13}C-enriched cultures were started by inoculating LB (^{12}C media) and Isogro media (98.5% ^{13}C enriched; from Sigma-Aldrich) with *E. coli* (OP50). Cultures were grown for 16 hr at 37°C, harvested by centrifugation, washed, and then combined 1:1, by weight, in M9 buffer. This mixture was spread onto 15 cm agarose plates (1.5% agarose, 50 mM NaCl, 1 mM $CaCl_2$, 1 mM $MgSO_4$, and 25 mM KPO_4, pH 6.0 buffer). Agarose plates prevented bacterial growth and, thus, the incorporation of exogenous carbon. For labeling assays, 30,000 synchronized L1 larvae were prepared by bleaching gravid adults and allowing embryos to hatch in the absence of food (Van Gilst et al., 2005). 20–24 hr after bleaching, L1s were plated on mixed isotope feeding plates and collected after 44–48 hr of feeding (worms were harvested as mid-L4 larvae). All experiments were carried out at 20°C.

Lipid Purification and Analysis

For whole-worm fatty acid analysis, total lipids were extracted and converted to fatty acid methyl esters (FAMEs) as described (Watts and Browse, 2002). For PL and TAG purification, total lipids were extracted with 2:1 chloroform:-methanol for 1 hr at room temperature. Next, 0.2 volumes of 0.9% NaCl were added and the mixture was vortexed and allowed to separate for 2 min. The top layer was removed and the bottom layer was dried down under nitrogen. Dried lipids were resuspended in 1 ml of chloroform. Calibrated phospholipid standard (1,2-Dihepatdecanoyl-*sn*-Glycero-3-Phosphocholine, Avanti Polar Lipids) and TAG standard (tritridecanoin, Nu-Chek Prep) were added to the total lipid mixture before extraction. PLs and TAGs were purified by solid phase exchange (SPE) chromatography. Extracted lipid was resuspended in chloroform and loaded onto SPE columns (100 mg capacity, Fisher Scientific) pre-equilibrated with 3 ml of chloroform. TAGs were eluted first with 3 ml of chloroform. Glycosphingolipids were eluted next with 5 ml of a 9:1 acetone:methanol mixture, and phospholipids were eluted last with 3 ml of methanol. Purified lipids were dried, resuspended in methanol/2.5% H_2SO_4, and incubated for 1 hr at 80°C to create FAMEs.

FAMEs were analyzed by gas chromatography/mass spectrometry (GC/MS) (Agilent 5975GC, 6920MS). Isotopomers were monitored in a scanning ion mode customized to each fatty acid species of interest; for example, C16:0 MS scans ranged from m/z = 265 to m/z = 290. To quantify TAG and PL yields, total PL and TAG were compared to the internally added standards. Data were presented as a TAG:PL ratio, which was determined by measuring the sum of all fatty acids found in TAGs versus the sum of all fatty acids found in PLs (Ashrafi et al., 2003).

Evaluation of Feeding Plate Isotope Composition, Enrichment, and Purity

For each experiment, the isotope composition of the feeding plates was independently characterized. To do this, a portion of the 1:1 feeding mixture was allocated to a "control" feeding plate. This plate was incubated at 20°C in the absence of worms for the entire course of the experiment. Bacteria were collected from these control feeding plates, and total lipid was extracted, transmethylated, and analyzed by GC/MS according to the same procedures described above.

We also used the feeding plate GC/MS data to calculate the relative ratio of labeled to unlabeled bacterial fatty acid on each set of feeding plates. Although we were careful in our efforts to mix bacteria equally by weight, we found that our cultures were generally not composed of an exact 1:1 mixture. The ratio of fully labeled to fully unlabeled palmitate was often skewed such that there was a slightly higher supply of unlabeled fatty acids, relative to labeled fatty acids (Figure 1B). For this reason, it was necessary for us to quantify the isotope composition of the bacterial mixture on each set of feeding plates. This information was used to establish a correction factor (CF) for calculations described below.

Calculating the Biosynthetic Origins of Palmitate

To model the mass spectra data, we developed mathematical terms to account for four potential origins of fatty acids in *C. elegans*: (1) de novo fatty acid synthesis, (2) direct dietary absorption, (3) absorption and elongation of dietary fatty acid, and (4) maternal inheritance. For palmitate methyl esters, we used Equation 1 to model total isotopomer abundance.

$$I_n(Tot) = I_n(Synth) + I_n(Abs) + I_n(Elong) + I_n(Mat), \mathrm{n} = 270, \ldots, 286 \quad (1)$$

where I_n is equal to isotopomers with a MW of n Daltons. $I_n(Tot)$ represents total abundance of each isotopomer. $I_n(Synth)$ equals the abundance of isotopomers resulting from de novo synthesis. $I_n(Abs)$ is equal to isotopomers resulting from directly absorbed C16:0. $I_n(Elong)$ represents isotopomers that were generated by elongation of dietary C14:0, and $I_n(Mat)$ takes into account fatty acids supplied by maternal contribution.

Corrections for ^{12}C Isotope Impurity in Labeled Media and Natural ^{13}C Abundance

To begin our analysis, we first determined the abundance of isotopomers due to isotope impurities. Impurity abundance was calculated for I_{271}, I_{272}, I_{273}, I_{283}, I_{284}, and I_{285} using standard binomial distributions (Kelleher, 2001). For our calculations, we used 1.11% as the natural ^{13}C abundance in the unlabeled fatty acids, and 1.5% as the ^{12}C contamination in the labeled fatty acids (See above and Figure 1B). Isotopomer abundance resulting from isotope impurity was then subtracted from the data in order to perform the calculations described below. At the end of our analysis, when $I_n(Abs)$, $I_n(Elong)$, $I_n(Synth)$, and $I_n(Mat)$ were determined, isotopomer impurity abundances were then assigned to each of the above terms and added back to create the final model (Figure 2A). Isotope impurity corrections were not used for isotopomers between 273 and 283 Daltons because the probability of obtaining a dietary fatty acid with MWs in this range is insignificant (Figure 1B) and because isotopomer peaks resulting from fatty acid synthesis are modeled by acetyl-CoA composition calculations, which take into account both isotope dilution and isotope impurity (see below).

Determining $I_n(Synth)$: Isotopomer Abundance due to Fatty Acid Synthesis

To model the contribution of de novo synthesis to C16:0 isotopomer abundance, we considered that C16:0 will be synthesized from eight acetyl-CoAs, and that these two-carbon substrates will be composed of ^{12}C-^{12}C, ^{12}C-^{13}C, or ^{13}C-^{13}C. Therefore, the MW of a synthesized C16:0 molecule will depend on the specific number of (^{12}C-^{12}C) substrates, (^{12}C-^{13}C) substrates, and ^{13}C-^{13}C substrates, termed A, B, and C, respectively, incorporated into that molecule. Since a total of eight two-carbon units are used to synthesize a C16:0 molecule, the specific number of each substrate will range from 0 to 8, and the sum of A, B, and C must be 8. Thus, a population of synthesized C16:0 will yield an isotopomer distribution that depends on the relative fractions of ^{12}C-^{12}C, ^{13}C-^{12}C, and ^{13}C-^{13}C substrates. The following trinomial expression was used to model the isotopomer distribution:

$$P(\mathrm{A},\mathrm{B},\mathrm{C}) = \left(\frac{8!}{A!B!C!}\right) P_a^A P_b^B P_c^C \quad (2)$$

where P_a equals the probability of incorporating a [^{12}C-^{12}C], P_b equals the probability of incorporating a [^{13}C-^{12}C], and P_c equals the probability of incorporating a [^{13}C-^{13}C]. Although P_a, P_b, and P_c could be theoretically determined by fitting the isotopomer data, we were able to experimentally measure these values directly by examining the elongation of C16:0 to C18:0 (see next section). Next, the probability of each combination of A, B, and C was determined and used to calculate the probability of obtaining isotopomers (P_n) from 270 to 286 Daltons.

$$P_n = \sum_n P(A,B,C), \text{ where } \mathrm{n} = 270 + (\mathrm{B} + 2\mathrm{C}) \quad (3)$$

These probabilities were then used to model the contribution of de novo synthesis to the isotopomer distribution using the following equation:

$$I_n(Synth) = (NF * P_n) \quad (4)$$

where P_n represents the probability of obtaining an isotopomer with MW n, and NF is a normalization factor that translates the probability of obtaining each isotopomer into total isotopomer abundance. The NF was determined by the following equation:

$$NF = I_{276}(Tot)/P_{276} \quad (5)$$

The I_{276} peak was used for normalization because this isotopomer is exclusively derived from synthesized fatty acid molecules; therefore $I_{276}(Tot)$ is equal to $I_{276}(Synth)$. Because our feeding mixture generally contained higher levels of ^{12}C bacteria and because worms also carried ^{12}C derived from the mother, two carbon units carried a disproportional amount of ^{12}C, causing the synthesis distributions to be skewed toward "lighter" isotopomers. This was well modeled by our analysis (Figure 2A). Importantly, our data were also well modeled using experimental determination of P_a, P_b, and P_c. The ability of experimentally measured probability values to correctly fit our synthesis data provides independent confirmation of the analysis.

Modeling $I_n(Elong)$: The Contribution of Dietary Fat Elongation to Isotopomer Abundance

In our palmitate mass spectra, even after removal of peaks due to isotope impurity, we consistently observed peaks at 272 and 284 Daltons that were significantly bigger than would be expected from synthesized palmitate (see Figure 2A). We deduced that these peaks resulted from elongation of dietary C14:0, a fatty acid species found in the *E. coli* diet (Table S1). Since this event must take place in *C. elegans,* elongation could occur with labeled, partially labeled, or unlabeled two-carbon units (see Figure S1). Palmitate molecules created by elongation of dietary C14:0 would thus yield isotopomers of 270, 271, and 272 (if an unlabeled C14:0 is elongated) or 284, 285, and 286 (if a labeled C14:0 is elongated). The accumulation of fatty acid synthesis-independent isotopomers at 282 Daltons was insignificant, suggesting that elongation of dietary C12:0 is not a major contributor to *C. elegans* palmitate. To calculate the contribution of C14:0 elongation to the palmitate isotopomer distribution, we first quantified the elongation of fully labeled C14:0 to C16:0 (Equation 6).

$$I_{284}(Elong) = I_{284}(Tot) - I_{284}(Synth) - I_{284}(Abs) \quad (6)$$

Because dietary palmitate (when isotope impurity peaks are removed) will not contribute isotopomers of 284 Daltons, $I_{284}(Abs)$ can be dropped from this equation. Next, $I_{285}(Elong)$ and $I_{286}(Elong)$ can be calculated using the relative abundance of [^{12}C-^{12}C], [^{13}C-^{12}C or ^{12}C-^{13}C], and [^{13}C-^{13}C] substrates available for elongation (Equations 7 and 8).

$$I_{285}(Elong) = I_{284}(Elong) * (P_b/P_a) \quad (7)$$

$$I_{286}(Elong) = I_{284}(Elong) * (P_c/P_a) \quad (8)$$

where P_a is the probability of elongating with a [^{12}C-^{12}C] substrate, P_b is the probability of elongating with a [^{13}C-^{12}C or ^{12}C-^{13}C] substrate, and P_c is the probability of elongating with a [^{13}C-^{13}C] substrate. The same methodology is used to calculate the abundance of I_{270}, I_{271}, and I_{272} isotopomers due to elongation of unlabeled C14:0. In this case, we use I_{272} abundance (after correction for isotope impurities) to calculate I_{271} and I_{270}.

Modeling $I_n(Abs)$: The Contribution of Dietary Palmitate Absorption

After taking into account synthesized fatty acids and elongated C14:0, the remainder of isotopomer abundance at I_{286} is attributable to the direct absorption of fully labeled dietary C16:0 (the probability of obtaining an isotopomer of 286 Daltons via fatty acid synthesis is extremely low, so this term can be excluded from the equation).

$$I_{286}(Abs) = I_{286}(Tot) - I_{286}(Elong) \quad (9)$$

Because maternal inheritance of C16:0 contributes to isotopomers at I_{270}, we cannot use the same formula to calculate $I_{270}(Abs)$. However, we can determine the amount of dietary fat at 270 Daltons using the relative proportion of labeled to unlabeled palmitate available to *C. elegans* (as determined in our analysis of the bacterial culture described above).

$$I_{270}(Abs) = I_{286}(Abs) * CF \quad (10)$$

The assumption in this case is that the amount of labeled and unlabeled fatty acids absorbed by *C. elegans* will be proportional to the relative abundance of labeled and unlabeled fatty acids in the diet. This ratio is determined by analyzing the bacterial feeding plate in order to obtain a CF. This CF is obtained by calculating the ratio of ^{12}C-labeled palmitate to ^{13}C-labeled palmitate in the mixed isotope bacterial cultures (see Figure 1B).

Modeling $I_n(Mat)$: The Contribution of Maternal Fatty Acid

After accounting for the above three factors, there was a remaining fraction of C16:0 abundance at 270 Daltons, i.e., fully unlabeled fatty acid. Since our worm growths were initiated by placing L1 larvae on mixed label feeding plates, some of the biomass in these L1 larvae may persist into the L4 stage of development. As L1 larvae biomass is entirely derived from unlabeled mothers, maternally contributed fatty acid must be completely unlabeled. Therefore, we concluded that the remaining fatty acid at 270 Daltons (generally around 5% of total fatty acid) was due to maternal contribution.

$$I_{270}(Mat) = I_{270}(Tot) - I_{270}(Abs) - I_{270}(Elong) - I_{270}(Synth) \quad (11)$$

As an independent means of calculating maternal contribution we transferred L1 larvae, which were hatched in the absence of food, to fully labeled ^{13}C bacteria. In this assay, any new fatty acids generated during the feeding period will contain ^{13}C isotope and therefore possess an MW greater than 270 Daltons. The amount of palmitate remaining at 270 Daltons was then determined at different time points during development as an indicator of maternally contributed fatty acid. Our data confirm that, by the L4 stage of development, the maternal contribution of palmitate is generally around 5% of total palmitate (see Figure S2). This provides a very satisfying secondary confirmation of our data analysis.

Experimental Determination of Acetyl-CoA Isotope Composition

In principle, the acetyl-CoA isotope composition could be obtained by fitting fatty acid synthesis data with a trinomial distribution while allowing the acetyl-CoA isotope composition to vary. However, we chose to experimentally assess isotope composition. The *E. coli* (OP50) diet of *C. elegans* contains insignificant levels of stearate (C18:0). Therefore, the primary means by which *C. elegans* obtains C18:0 is by elongation of C16:0. We exploited this property to calculate the isotope composition of acetyl-CoA units for each experiment (Figures 2B and 2C). If a fully labeled C16:0 is elongated to stearate in *C. elegans*, the MW of stearate will directly reflect the fractions of ^{12}C-^{12}C, ^{13}C-^{12}C, and ^{13}C-^{13}C. Thus, by quantifying the abundance of C18:0 (I_{314}), C18:0 (I_{315}), and C18:0 (I_{316}), we can determine the probability of incorporating the different isotopomers of acetyl-CoA (Equations 12–14). These numbers were calculated after correction for isotope impurity.

$$P_a = I_{314}(Tot)/(I_{314}(Tot) + I_{315}(Tot) + I_{316}(Tot)) \quad (12)$$

$$P_b = I_{315}(Tot)/(I_{314}(Tot) + I_{315}(Tot) + I_{316}(Tot)) \quad (13)$$

$$P_c = I_{316}(Tot)/(I_{314}(Tot) + I_{315}(Tot) + I_{316}(Tot)) \quad (14)$$

where P_a equals the probability of incorporating a [^{12}C-^{12}C], P_b equals the probability of incorporating a [^{12}C-^{13}C or ^{13}C-^{12}C], and P_c equals the probability of incorporating a [^{13}C-^{13}C]. The fact that this method for determining acetyl-CoA isotope composition produced models that correctly predicted both synthesized and elongated isotopomer distribution in C16:0 independently confirms our analyses and also argues that the same pool of acetyl-CoA is used for elongation and for de novo synthesis.

Determination of Synthesis Levels for Other Fatty Acids in WT and Mutant Strains

For the majority of our study, we present data as the fraction of fatty acid that was generated through de novo synthesis. This number was expressed as the total amount of synthesized fatty acid over the total dietary fatty acid taken up or synthesized during the feeding assay. Equation 15 represents the method used to calculate percent synthesis.

$$\%\ \text{FA Synthesis} = \frac{\sum_{270}^{286} I_n(Synth)}{\sum_{270}^{286} I_n(Tot) - I_{270}(Mat)} * 100 \quad (15)$$

For all fatty acid species, the trinomial distribution described in the previous section was used to calculate total fatty acid synthesis. For 18 carbon fatty acids, we used a trinomial distribution that accounted for the assembly of nine acetyl-CoA units.

SUPPLEMENTAL DATA

Supplemental Data include three figures and one table and can be found with this article online at http://www.cellmetabolism.org/cgi/content/full/8/3/266/DC1/.

ACKNOWLEDGMENTS

We thank the Caenorhabditis Genetics Center for supplying *C. elegans* strains. We thank Nick Terzopoulos and Felix Nau, Jr. for assistance with worm maintenance and media preparation. We also acknowledge Dan Gottschling, David Hockenberry, Eric Foss, Rich Van Gilst, and WenYing Shou for comments on the manuscript and members of the Van Gilst laboratory for useful discussions. C.L.P. is supported in part by PHS NRSA T32 GM07270. M.R.V.G. is supported by the American Diabetes Association (1-07-JF-72).

Received: April 16, 2008
Revised: July 25, 2008
Accepted: August 12, 2008
Published: September 2, 2008

REFERENCES

Ashrafi, K., Chang, F.Y., Watts, J.L., Fraser, A.G., Kamath, R.S., Ahringer, J., and Ruvkun, G. (2003). Genome-wide RNAi analysis of Caenorhabditis elegans fat regulatory genes. Nature *421*, 268–272.

Bluher, M., Michael, M.D., Peroni, O.D., Ueki, K., Carter, N., Kahn, B.B., and Kahn, C.R. (2002). Adipose tissue selective insulin receptor knockout protects against obesity and obesity-related glucose intolerance. Dev. Cell *3*, 25–38.

Brunengraber, H., Kelleher, J.K., and Des Rosiers, C. (1997). Applications of mass isotopomer analysis to nutrition research. Annu. Rev. Nutr. *17*, 559–596.

Bruning, J.C., Michael, M.D., Winnay, J.N., Hayashi, T., Horsch, D., Accili, D., Goodyear, L.J., and Kahn, C.R. (1998). A muscle-specific insulin receptor knockout exhibits features of the metabolic syndrome of NIDDM without altering glucose tolerance. Mol. Cell *2*, 559–569.

Bruning, J.C., Gautam, D., Burks, D.J., Gillette, J., Schubert, M., Orban, P.C., Klein, R., Krone, W., Muller-Wieland, D., and Kahn, C.R. (2000). Role of brain insulin receptor in control of body weight and reproduction. Science *289*, 2122–2125.

Gems, D., Sutton, A.J., Sundermeyer, M.L., Albert, P.S., King, K.V., Edgley, M.L., Larsen, P.L., and Riddle, D.L. (1998). Two pleiotropic classes of daf-2 mutation affect larval arrest, adult behavior, reproduction and longevity in Caenorhabditis elegans. Genetics *150*, 129–155.

Halaschek-Wiener, J., Khattra, J.S., McKay, S., Pouzyrev, A., Stott, J.M., Yang, G.S., Holt, R.A., Jones, S.J., Marra, M.A., Brooks-Wilson, A.R., and Riddle, D.L. (2005). Analysis of long-lived C. elegans daf-2 mutants using serial analysis of gene expression. Genome Res. *15*, 603–615.

Hellerer, T., Axang, C., Brackmann, C., Hillertz, P., Pilon, M., and Enejder, A. (2007). Monitoring of lipid storage in Caenorhabditis elegans using coherent

anti-Stokes Raman scattering (CARS) microscopy. Proc. Natl. Acad. Sci. USA *104*, 14658–14663.

Holzenberger, M., Dupont, J., Ducos, B., Leneuve, P., Geloen, A., Even, P.C., Cervera, P., and Le Bouc, Y. (2003). IGF-1 receptor regulates lifespan and resistance to oxidative stress in mice. Nature *421*, 182–187.

Katic, M., Kennedy, A.R., Leykin, I., Norris, A., McGettrick, A., Gesta, S., Russell, S.J., Bluher, M., Maratos-Flier, E., and Kahn, C.R. (2007). Mitochondrial gene expression and increased oxidative metabolism: role in increased lifespan of fat-specific insulin receptor knock-out mice. Aging Cell *6*, 827–839.

Kelleher, J.K. (2001). Flux estimation using isotopic tracers: common ground for metabolic physiology and metabolic engineering. Metab. Eng. *3*, 100–110.

Kelleher, J.K. (2004). Probing metabolic pathways with isotopic tracers: insights from mammalian metabolic physiology. Metab. Eng. *6*, 1–5.

Kenyon, C., Chang, J., Gensch, E., Rudner, A., and Tabtiang, R. (1993). A C. elegans mutant that lives twice as long as wild type. Nature *366*, 461–464.

Kniazeva, M., Crawford, Q.T., Seiber, M., Wang, C.Y., and Han, M. (2004). Monomethyl branched-chain fatty acids play an essential role in Caenorhabditis elegans development. PLoS Biol. *2*, E257. 10.1371/journal.pbio.0020257.

Lee, R.Y., Hench, J., and Ruvkun, G. (2001). Regulation of C. elegans DAF-16 and its human ortholog FKHRL1 by the daf-2 insulin-like signaling pathway. Curr. Biol. *11*, 1950–1957.

McCabe, B.J., and Previs, S.F. (2004). Using isotope tracers to study metabolism: application in mouse models. Metab. Eng. *6*, 25–35.

McElwee, J., Bubb, K., and Thomas, J.H. (2003). Transcriptional outputs of the Caenorhabditis elegans forkhead protein DAF-16. Aging Cell *2*, 111–121.

McElwee, J.J., Schuster, E., Blanc, E., Thornton, J., and Gems, D. (2006). Diapause-associated metabolic traits reiterated in long-lived daf-2 mutants in the nematode Caenorhabditis elegans. Mech. Ageing Dev. *127*, 458–472.

Min, K.J., Hogan, M.F., Tatar, M., and O'Brien, D.M. (2006). Resource allocation to reproduction and soma in Drosophila: a stable isotope analysis of carbon from dietary sugar. J. Insect Physiol. *52*, 763–770.

Mukhopadhyay, A., Deplancke, B., Walhout, A.J., and Tissenbaum, H.A. (2005). *C. elegans* tubby regulates life span and fat storage by two independent mechanisms. Cell Metab. *2*, 35–42.

Murphy, C.T., McCarroll, S.A., Bargmann, C.I., Fraser, A., Kamath, R.S., Ahringer, J., Li, H., and Kenyon, C. (2003). Genes that act downstream of DAF-16 to influence the lifespan of Caenorhabditis elegans. Nature *424*, 277–283.

Murphy, E.J. (2006). Stable isotope methods for the in vivo measurement of lipogenesis and triglyceride metabolism. J. Anim. Sci. *84* (*Suppl*), E94–E104.

O'Brien, D.M., Min, K.J., Larsen, T., and Tatar, M. (2008). Use of stable isotopes to examine how dietary restriction extends *Drosophila* lifespan. Curr. Biol. *18*, R155–R156.

Ogg, S., Paradis, S., Gottlieb, S., Patterson, G.I., Lee, L., Tissenbaum, H.A., and Ruvkun, G. (1997). The Fork head transcription factor DAF-16 transduces insulin-like metabolic and longevity signals in C. elegans. Nature *389*, 994–999.

Patel, D.S., Garza-Garcia, A., Nanji, M., McElwee, J.J., Ackerman, D., Driscoll, P.C., and Gems, D. (2008). Clustering of genetically defined allele classes in the Caenorhabditis elegans DAF-2 insulin/IGF-1 receptor. Genetics *178*, 931–946.

Strawford, A., Antelo, F., Christiansen, M., and Hellerstein, M.K. (2004). Adipose tissue triglyceride turnover, de novo lipogenesis, and cell proliferation in humans measured with 2H2O. Am. J. Physiol. Endocrinol. Metab. *286*, E577–E588.

Sze, J.Y., Victor, M., Loer, C., Shi, Y., and Ruvkun, G. (2000). Food and metabolic signalling defects in a Caenorhabditis elegans serotonin-synthesis mutant. Nature *403*, 560–564.

Van Gilst, M.R., Hadjivassiliou, H., Jolly, A., and Yamamoto, K.R. (2005). Nuclear hormone receptor NHR-49 controls fat consumption and fatty acid composition in C. elegans. PLoS Biol. *3*, e53. 10.1371/journal.pbio.0030053.

Watts, J.L., and Browse, J. (2002). Genetic dissection of polyunsaturated fatty acid synthesis in Caenorhabditis elegans. Proc. Natl. Acad. Sci. USA *99*, 5854–5859.

Wolkow, C.A., Kimura, K.D., Lee, M.S., and Ruvkun, G. (2000). Regulation of C. elegans life-span by insulinlike signaling in the nervous system. Science *290*, 147–150.